Title

Receptor Level Mechanisms Are Required for Epidermal Growth Factor (EGF)-stimulated Extracellular Signal-regulated Kinase (ERK) Activity Pulses*

Journal

Journal of Biological Chemistry, 290(41)

ISSN

0021-9258

Authors

Sparta, Breanne
Pargett, Michael
Minguet, Marta
et al.

Publication Date

2015-10-01

DOI

10.1074/jbc.m115.662247

Peer reviewed

THE JOURNAL OF BIOLOGICAL CHEMISTRY VOL. 290, NO. 41, pp. 24784–24792, October 9, 2015

Receptor Level Mechanisms Are Required for Epidermal Growth Factor (EGF)-stimulated Extracellular Signal-regulated Kinase (ERK) Activity Pulses*

Received for publication, May 7, 2015, and in revised form, August 14, 2015 Published, JBC Papers in Press, August 24, 2015, DOI 10.1074/jbc.M115.662247

Breanne Sparta[‡], Michael Pargett[‡], Marta Minguet[‡], Kevin Distor[‡], George Bell[§], and John G. Albeck[‡1]

From the Departments of [‡]Molecular and Cellular Biology and [§]Microbiology and Molecular Genetics, University of California, Davis, California 95616

Background: In individual cells, EGF stimulation results in sporadic pulses of ERK activity.
Results: ERK pulses are disrupted upon stimulation by alternate receptors or inhibition of EGFR.
Conclusion: ERK activity pulses are generated at the level of EGFR.
Significance: The dynamics of ERK activity, which control cellular proliferation and gene expression, are inconsistent with models that rely on downstream feedback.

In both physiological and cell culture systems, EGF-stimulated ERK activity occurs in discrete pulses within individual cells. Many feedback loops are present in the EGF receptor (EGFR)-ERK network, but the mechanisms driving pulsatile ERK kinetics are unknown. Here, we find that in cells that respond to EGF with frequency-modulated pulsatile ERK activity, stimulation through a heterologous TrkA receptor system results in non-pulsatile, amplitude-modulated activation of ERK. We further dissect the kinetics of pulse activity using a combination of FRET- and translocation-based reporters and find that EGFR activity is required to maintain ERK activity throughout the 10–20-minute lifetime of pulses. Together, these data indicate that feedbacks operating within the core Ras-Raf-MEK-ERK cascade are insufficient to drive discrete pulses of ERK activity and instead implicate mechanisms acting at the level of EGFR.

The EGF-Ras-ERK signaling pathway (Fig. 1*A*) controls cell proliferation, survival, migration, and differentiation. The terminal kinase ERK phosphorylates >100 substrates (1), and the dynamics of ERK activity determine cellular phenotype. In the PC-12 cell line, a widely used model for ERK regulation, stimulation with EGF results in transient ERK activity that efficiently stimulates cell cycle entry and proliferation, whereas NGF stimulates sustained ERK activity that drives differentiation (2). Many ERK target genes, including c-Fos and c-Myc, are sensitive to ERK kinetics because ERK activity is required for both transcription and stabilization of the gene products (3, 4). Cell cycle entry is similarly sensitive, requiring ERK activity during specific periods of competence where the appropriate substrates are present (5, 6). The intensity (or amplitude) of ERK activity can also determine cellular outcome; cell cycle entry and protection from apoptosis require different threshold levels of ERK activity in melanoma cells (7). Thus, accurately measuring ERK activation kinetics and intensity is essential to understanding its physiological function.

A challenge in measuring ERK kinetics lies in the use of population level measurements, such as immunoblotting, where data points represent the average of 10^4 to 10^8 cells. Such measurements are degenerate with respect to the states of individual cells because multiple scenarios could give rise to the same population average (*e.g.* a change in each cell's intensity *versus* a change in the frequency of "on" *versus* "off" cells) (8). The mean of a population is often a poor descriptor of any individual cell, particularly when cells exist in two or more distinct groups with different properties. Fixed single-cell methods, such as immunofluorescence, may also fail to resolve these situations because measurement noise and cellular variability can falsely create the appearance of a bimodal population (9). To address these problems, live cell reporters for ERK pathway activity have been developed, allowing individual cells to be tracked continuously (10–13) and eliminating the inference steps required to interpret population level or fixed single-cell data.

ERK activity occurs in discrete pulses that are similar in amplitude, regardless of the strength of stimulus, in single cells responding to physiological levels of EGF or to serum (12–14). Although these pulses occur sporadically with no fixed period, their frequency increases with the concentration of EGF ligand (13) and is driven in part by autocrine signaling (14, 15). ERK pulses occur in multiple cell lines and *in vivo* as well (14, 15), suggesting that they are a physiologically relevant mode of signaling. This form of regulation, also found in other signaling pathways (16, 17), has been referred to as "frequency modulation" (Fig. 1*B*) because it is the frequency rather than the amplitude of the discrete pulses that responds to and encodes the strength of the extracellular stimulus. In contrast, an "amplitude-modulated" response changes in intensity as a function of the upstream stimulus (Fig. 1*B*).

A linear signaling pathway with no feedback would be expected to be amplitude-modulated. Discrete activity pulses with similar amplitude generally require both positive feedback to enforce the stimulus-independent transition to the "on" state

* This work was supported in part by the American Cancer Society (IRG-95-125-16). The authors declare that they have no conflicts of interest with the contents of this article.
[1] To whom correspondence should be addressed: Dept. of Molecular and Cellular Biology, University of California, Davis, One Shields Ave., Davis, CA 95616. Tel.: 530-752-0646; E-mail: jgalbeck@ucdavis.edu.

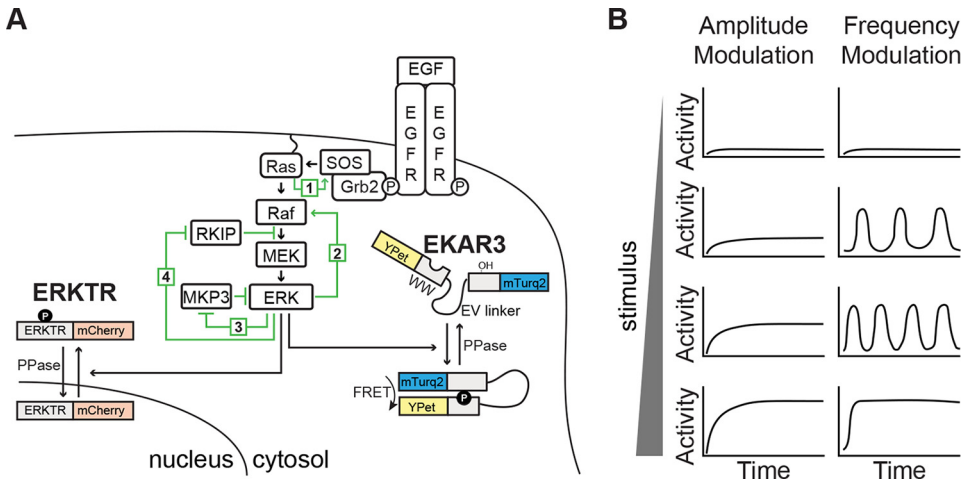

FIGURE 1. **Encoding of extracellular signal strength by the ERK network.** *A*, schematic diagram of EGFR-ERK signaling system and reporter readouts. *Green arrows* indicate potential positive feedback loops. *B*, conceptual comparison of amplitude- and frequency-modulated signal responses.

and negative feedback with a delay to drive a return to "off." Although negative feedbacks in EGFR[2] signaling have been compared quantitatively (18), it is not clear which positive feedback loops are involved. Within the ERK pathway, there are at least four positive feedbacks that have been identified: 1) allosteric activation of SOS by GTP-bound Ras (19, 20), 2) stimulatory phosphorylation of Raf by ERK (21), 3) phosphorylation-induced degradation of the MKP-3 phosphatase (22), or 4) inhibitory phosphorylation of the negative Raf-MEK regulator RKIP by ERK (23) (see corresponding *green arrows* in Fig. 1*A*). Although many of these features have been shown to be capable of creating either pulselike or oscillatory behavior in mathematical simulations (14, 23, 24), the question of which feedbacks operate *in vivo* to create spontaneous ERK activity pulses remains unanswered.

Here, we asked whether frequency-modulated signaling is dependent on events occurring at the EGF receptor. Because MCF10A mammary epithelial cells exhibit robust frequency-modulated ERK activity in response to EGF but do not respond to NGF, we tested whether heterologous expression of TrkA would result in an amplitude- or frequency-modulated response to increasing doses of NGF. In contrast to the EGF response, we found that the NGF-TrkA system induces amplitude-modulated ERK activation, implicating EGFR-specific events as critical for pulse generation. To confirm this idea, we monitored EGFR inhibition using a dual-reporter system to achieve high temporal resolution and found that termination of EGFR activity was capable of prematurely arresting ERK activity mid-pulse. These data indicate that a non-linear process operating at the receptor level is required for ERK activity pulses induced by EGF.

Experimental Procedures

Culture Media and Reagents—MCF10A-5e cells were maintained as described previously (25). Culture media were obtained from Life Technologies; bovine serum albumin, hydrocortisone, cholera toxin, and insulin from Sigma; EGF and NGF from Peprotech; and gefitinib from Selleck.

Plasmid and Cell Line Construction—To construct EKAR3, we used PCR and restriction cloning to insert restriction sites into pPB-CAG-EKAREV-nes (a gift from K. Aoki and M. Matsuda) between all major reporter elements, resulting in pPBJ-EKAR-EV-nes. We then replaced the SECFP donor fluorescent protein with the sequence of mTurquoise2 (Addgene, catalog no. 36201) by restriction digest and ligation, resulting in pPBJ-EKAR3-nes. Cells stably expressing EKAR3 or EKAR-EV were derived through co-transfection of pPBJ-EKAR-EV-nes or pPBJ-EKAR3-nes and the pCMV-hyPBase transposase vector. pMSCV-puro-ERKTR-mCherry was constructed by ligating the coding sequences for residues 1–82 of ERKTR (12) and mCherry red fluorescent protein into pMSCV-puro. Retroviral particles carrying ERKTR-mCherry were produced by co-transfecting 293T cells with pMSCV-puro-ERKTR-mCherry and pCL-Ampho and used to infect MCF10A-EKAR3 cells, resulting in co-expression of EKAR3 and ERKTR-mCherry. pLT-NTRK1-IRES-NLS-mCherry was created by cloning an SV40 nuclear localization sequence into the N terminus of mCherry, followed by the sequential ligation of NLS-mCherry and NTRK1 into the pLT-IRES vector. NTRK1 DNA was cloned into pLT-IRES-Neo downstream of the Tet-responsive promoter, whereas NLS-mCherry was ligated downstream of the hepatitis C virus internal ribosome entry site (IRES). Cell lines stably expressing NTRK1 were generated by lentiviral infection and isolation of Geneticin-resistant colonies. Monoclonal cell lines were obtained by limited dilution cloning.

Live Cell Imaging—Time lapse imaging was performed using a Nikon TiE equipped with automated stage and filter turret and an environmental chamber. Images were obtained with a ×20, 0.75 numerical aperture plan apochromat objective and recorded with an Andor Zyla scMOS camera, using Nikon Elements software. The following filter sets were used: CFP, Chroma 49001; YFP, Chroma 49003; RFP, Chroma 41043 or Semrock FF03-575/25-25, FF01-640/40-25, FF605-Di02-25x36. For imaging, cells were plated on number 1.5 glass bottom 96- or 24-well plates (In Vitro Scientific) coated with Type I collagen (BD Biosciences) and maintained at 37 °C in 5% CO_2.

[2] The abbreviations used are: EGFR, EGF receptor; IRES, internal ribosome entry site; TrkA, tyrosine receptor kinase A; EKAR, ERK kinase activity reporter; ERKTR, ERK translocation reporter; pERK, phosphorylated ERK; CFP, cyan fluorescent protein.

At least 6 h prior to imaging, growth medium was replaced with custom low fluorescence medium lacking serum and growth factors (DMEM/F-12 lacking phenol red, riboflavin, and folate (Life Technologies, Inc.), supplemented with 0.1% bovine serum albumin, 0.5 μg/ml hydrocortisone, 100 ng/ml cholera toxin, 50 units/ml penicillin, and 50 μg/ml streptomycin). Growth factor stimulation during imaging was performed by adding a 10- or 20-fold concentrated solution of growth factor, diluted in imaging medium, to achieve the desired concentration in each well on the multiwell imaging plate.

Image and Data Analysis—Raw image files were converted to TIFF format by Nikon Elements and then imported to MATLAB for image segmentation, tracking, and quantitation. A custom MATLAB routine was used to identify cells based on the cytosolic localization of EKAR3, containing a nuclear export sequence. Cell tracking was performed using the u-track algorithm (26). The nuclear region for each cell was defined by automated selection of edge-based contours using filters for size and circularity, and the cytosolic region was defined as a 7-pixel-wide annulus surrounding the nuclear region. EKAR-EV or EKAR3 signals were calculated as the average CFP/YFP ratio within the cytosolic region (a calculation that does not introduce non-linearity into the measurement, unlike the commonly used FRET/CFP ratio (27)). Because this ratio decreases as ERK activity increases, it is displayed linearly inverted by multiplying by −1 and adding a constant chosen to center the baseline near 0. ERKTR signal was calculated as the ratio of cytosolic to nuclear intensity for ERKTR-mCherry. All data shown are representative of at least three independent experiments, with >200 cells analyzed in each experiment.

Results

To track ERK activity in living cells, we developed an updated version of EKAR-EV, a genetically encoded FRET-based biosensor (10). To improve the signal/noise ratio, we replaced the enhanced CFP donor fluorophore with mTurquoise2, a CFP variant with a quantum yield of >90% (28). This reporter, which we term EKAR3, retains the linker, phosphorylation site, and phosphobinding domain of EKAR-EV. MCF10A mammary epithelial cells clonally expressing EKAR3 (Fig. 2*A*) were exposed to 20 ng/ml EGF to induce a maximal response, followed by a MEK inhibitor, to establish the dynamic range of the reporter (Fig. 2*B*). In comparison with EKAR-EV, EKAR3 had a smaller coefficient of variation (*CV*) between cells at both high and low levels of activity (Fig. 2*B*). In individual cells, the differential between high and low states had a 4.7-fold lower *CV* for EKAR3 relative to EKAR2. This improvement probably results from enhanced detection of the CFP donor relative to background fluorescence and makes it possible to more reliably distinguish different levels of ERK activation using the reporter.

To verify that this improved reporter allows observation of previously reported characteristics of ERK activity (13, 14), we imaged MCF10A-EKAR3 cells in serum-free, growth factor-free medium prior to and for 24 h following EGF stimulation (Fig. 2*C*), and we used automated image analysis to track >200 cells in each condition. To optimally display both single cell responses and population level trends, we utilized a system of three plots: two representative individual cell traces (Fig. 2*C*, *top row*), population mean, and 25th/75th percentile range overlaid against 50 individual traces (*middle row*) and a heat map with ERK activity represented as *color* (*bottom row*). Stimulation with 20 ng/ml EGF induced a rapid increase in the CFP/YFP signal that was sustained for the remainder of the experiment. Except for a small dip in activity between 6 and 12 h, essentially all cells maintained a high level of ERK activity. At a lower dose of EGF (0.1 ng/ml), an initial pulse of ERK activity upon treatment was followed by sporadic pulses for the remainder of a 24-h experiment, confirming frequency-modulated behavior. Most cells displayed at least 2–3, and typically >10 alternating intervals of high and low ERK activity (Fig. 2*C*, *bottom*). However, because these intervals were asynchronous, the mean population signal remained nearly constant for 24 h following stimulation (Fig. 2*C*, *middle*). In the absence of exogenous EGF addition, most cells maintained a low level of ERK activity (Fig. 2*C*, *top*), but we noted sporadic pulses of activity in some cells (Fig. 2*C*, *middle* and *bottom*); these rare pulses were eliminated in the presence of the EGFR inhibitor gefitinib (data

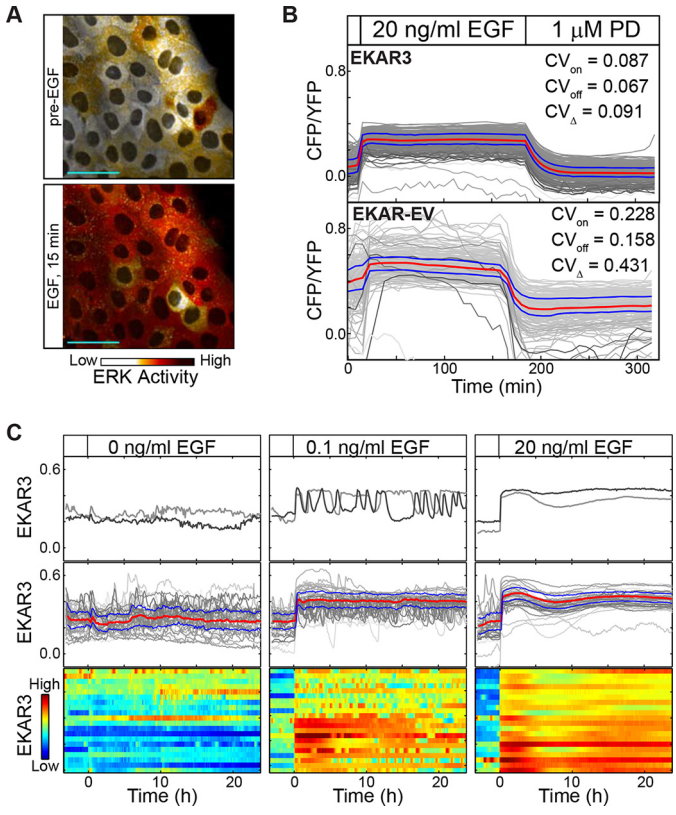

FIGURE 2. **EKAR3, an improved FRET reporter for detection of ERK activity.** *A*, ratiometric CFP/YFP images of MCF10A-EKAR3 cells before and after EGF (20 ng/ml) addition. *Scale bars*, 50 μm. *B*, comparison of EKAR3 and EKAR-EV reporter responses to saturating EGF (20 ng/ml) stimulation followed by MEK inhibition. CV_{on}, CV_{off}, and $CV\Delta$ indicate the coefficient of variation for cells in the EGF-stimulated state, cells in the MEK inhibited state, and the individual cell difference between the on and off state, respectively. Data shown were collected in MCF10A *FOSL1*::mCherry cells; mCherry fluorescence (not shown) does not interfere with the FRET signals. *C*, ERK response to different levels of EGF stimulation, as measured by EKAR3. MCF10A-EKAR3 cells were cultured in serum-free, growth factor-free imaging medium and then treated at the indicated time. Reporter data are displayed in three ways: two representative individual cells (*top*), 50 cell traces overlaid with the population mean in *red* and the 25th and 75th percentile values in blue (*middle*), and a heat map in which each *row* represents one cell and EKAR3 signal is indicated by *color* (*bottom*).

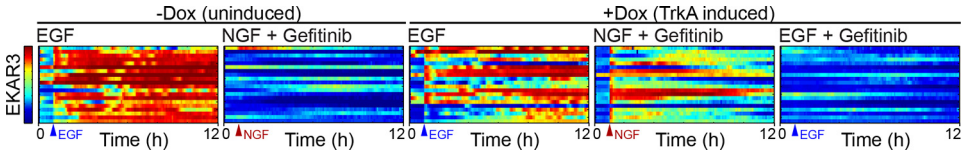

FIGURE 3. **Expression of TrkA confers NGF sensitivity to MCF10A cells.** MCF10A cells carrying an inducible TrkA gene were cultured in serum-free, growth factor-free medium in the absence or presence of 50 ng/ml doxycycline and then treated at the indicated time with 1 ng/ml EGF, 25 ng/ml NGF, or 1 μM gefitinib. EKAR3 responses are plotted as heat maps depicting a representative set of 20 cells for each condition.

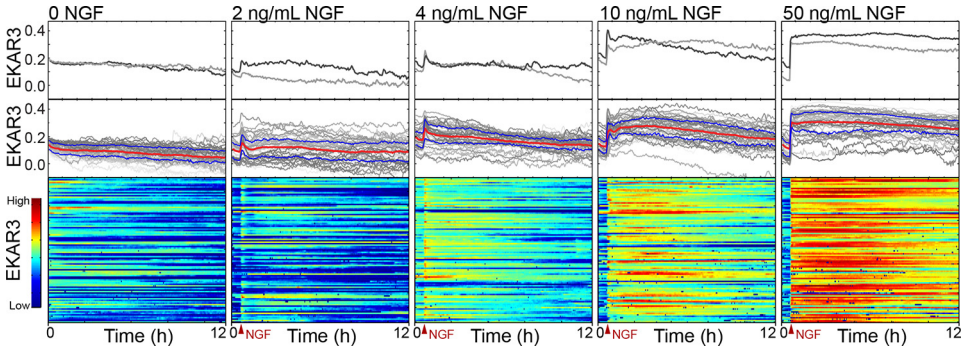

FIGURE 4. **Amplitude-modulated ERK signaling induced by NGF-TrkA.** MCF10A-EKAR3 cells expressing TrkA were cultured in serum-free, growth factor-free medium in the presence of 100 ng/ml doxycycline and then treated with the indicated concentrations of NGF at the times indicated by *arrowheads*. Data are plotted as in Fig. 2*C*.

not shown),[3] suggesting that they arise from autocrine signaling as reported previously (14).

EGFR activation is a complex process involving conformational changes (29) and a large number of distinct molecular complexes containing other ErbB family members and adaptor proteins (30). To determine whether frequency-modulated dynamics can be stimulated by a less complex receptor tyrosine kinase system, we turned to TrkA, a receptor tyrosine kinase that responds to NGF through induced receptor dimerization upon ligand binding (31). MCF10A cells express low or undetectable levels of TrkA and its potential heterodimerization partners TrkB and p75 (32, 33) and do not respond to NGF (Fig. 3). We stably integrated the NTRK1 cDNA encoding TrkA into MCF10A-EKAR3 cells under a doxycycline-regulated promoter. The NTRK1 sequence was followed by an IRES-mCherry cassette, allowing us to monitor the relative expression level of the receptor. Following treatment with doxycycline for 3 days to allow stable transgene expression, these cells became responsive to NGF with a robust, steady EKAR3 signal upon NGF treatment (Fig. 3). This EKAR3 response was not prevented by the specific EGFR inhibitor gefitinib, indicating that EGFR activity was not involved in ERK activation.

We next asked whether NGF-stimulated ERK activity displayed amplitude- or frequency-modulated characteristics. After stable induction of TrkA, we exposed these cells to NGF at concentrations ranging from 2 to 50 ng/ml (Fig. 4). At all concentrations, EKAR3 signal in individual cells rose within 6 min to reach a small peak before declining slightly to reach a level that was sustained for the duration of the 12-h experiment (Fig. 4, *top row*). The mean intensity of both the initial peak and the sustained EKAR3 signal increased monotonically with the concentration of NGF (Fig. 4, *middle row*). At the population level, the sustained intensity of EKAR3 signal varied from cell to cell, and some cells occasionally displayed small pulses of activity intermixed with the sustained activity (Fig. 4, *bottom row*). Overall, this pattern of induction contrasts with the activation pattern stimulated by increasing EGF doses (Fig. 2*C*) and fits the amplitude-modulated model (Fig. 1*B*).

Because EGFR and TrkA differ in the kinetics and configuration with which they recruit adaptor proteins and activate the small GTPases Ras and Rap (34, 35) but share the Raf-MEK-ERK cascade in common, the difference in ERK kinetics between EGFR- and TrkA-driven responses appears to originate at the level of receptor signaling complex assembly and not from feedback within the downstream cascade. Therefore, we speculated that the pulsatile ERK activity induced by EGF may depend on feedback or cooperativity that requires continued kinase activity of EGFR. A further test for such a model is whether already-initiated ERK pulses are sustained when EGFR kinase activity is terminated before the pulses reach their peak. If receptor level feedback or cooperativity is responsible for pulse generation, then initiated pulses would not reach their peak if receptor kinase activity ceases prematurely. Conversely, if positive feedback acts at a point downstream of the receptor, initiated pulses will become independent of EGFR and will reach maximum amplitude even in the presence of an EGFR inhibitor. This test requires temporal resolution sufficient to distinguish partial from full-amplitude peaks, which are typically reached within 10 min following initiation.

Recently, Covert and co-workers (12) described an alternative kinase reporter design, ERKTR, based on phosphorylation-stimulated nuclear/cytoplasmic translocation, with potentially more rapid kinetics than FRET-based reporters. To compare these kinetics directly, we co-expressed EKAR3 and ERKTR in MCF10A cells and imaged their behavior at 1.5-min intervals in cells upon stimulation with EGF (Fig. 5*A*, *left*) or treatment with EGFR inhibitor (Fig. 5*A*, *right*). Comparison of the mean signals for each reporter revealed multiple kinetic differences. First, the

[3] M. Minguet, K. Distor, and J. G. Albeck, unpublished data.

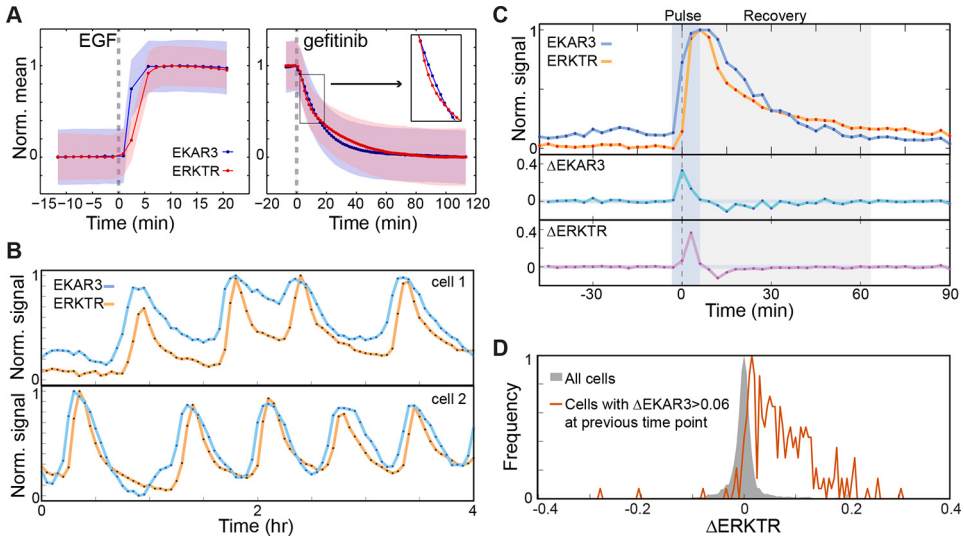

FIGURE 5. **Kinetic differences between EKAR3 and ERKTR.** *A*, comparison of EKAR3 and ERKTR responses to EGF stimulation (*left*) or EGFR inhibition (*right*). MCF10A cells stably expressing both reporters were imaged in the absence of growth factors and serum and then treated with 20 ng/ml EGF at time 0 (*left*) or cultured in 20 ng/ml EGF and treated with 1 μM gefitinib at time 0 (*right*). For each reporter, the mean signal of >200 cells, normalized to its minimum and maximum, is shown as a *line plot*; *shaded regions* indicate one S.D. The *inset* in the *right panel* highlights the more rapid decrease in ERKTR signal during the initial period of inhibition. *B*, comparison of EKAR3 and ERKTR-mCherry signals in two representative MCF10A cells expressing both reporters during spontaneous pulsing (under continuous treatment with 0.05 ng/ml EGF). Each reporter was normalized to its maximum and minimum value in each cell. *C*, detailed view of a single spontaneous ERK activity pulse detected by EKAR3 and ERKTR-mCherry. MCF10A-EKAR3-ERKTR cells were cultured continuously in the presence of 0.1 ng/ml EGF, and one cell with an isolated representative pulse was chosen for display. *Top panel*, reporter signals, normalized to the minimum and maximum for each signal. *Bottom panels*, frame-to-frame difference for each reporter signal. *D*, signature of pulse continuation in dual ERK reporter cells exposed continuously to 0.05 ng/ml EGF. Distributions represent the value of ΔERKTR at an arbitrarily chosen time point for all cells (*gray*) or for cells in which ΔEKAR3 was greater than the threshold value for pulse activity at the previous time point (*orange*). Frequency is normalized to its peak value.

rapid increase in EKAR3 upon EGF stimulation occurred ~2 min earlier than the corresponding increase in ERKTR. Second, the reporters showed different kinetics of deactivation upon EGFR inhibition. Initially, ERKTR signal decayed more rapidly than EKAR3 (Fig. 5*A*, *right*, *inset*). This difference is consistent with the idea that intramolecular binding of the WW domain to the phosphothreonine residue in EKAR3 prevents the efficient removal of the phosphate by phosphatases. However, at later times, EKAR3 reached its baseline level more rapidly than ERKTR; this effect may reflect the longer time required for the nuclear/cytosolic transport of the reporter to reach equilibrium than for the FRET reporter to make a conformational change.

We next compared EKAR3 and ERKTR kinetics during spontaneous ERK pulses induced by low concentrations of EGF. Overall, we observed a high degree of coincidence between the two reporters (Fig. 5*B*). Examination of individual pulses in detail (Fig. 5*C*) revealed differences in kinetics between the reporters that were consistent with the bulk analysis (Fig. 5*A*). EKAR3 rose ~2 min earlier than ERKTR during the initiation of the pulse, whereas ERKTR showed a more rapid initial decrease as the pulse dissipated (Fig. 5*C*). Overall, we find two potential advantages in the co-expressed reporter system: 1) a higher reliability of peak detection by cross-comparison of reporters and 2) increased resolution of the detection of both the increase in ERK activity (using EKAR3) and decrease (using ERKTR) within each pulse.

The difference in response kinetics between the two reporters suggested a means to evaluate the completion of initiated ERK pulses. We compared the frame-to-frame differential of each reporter (ΔEKAR3 and ΔERKTR, respectively; Fig. 5*C*) and found that because of the difference in activation rate, the maximum ΔEKAR3 typically preceded the maximum ΔERKTR by one frame when sampled at 3-min intervals. This shift created a detectable signature in time series from large numbers of cells; when a threshold value of ΔEKAR3 at frame t was set to identify cells in the early stage of a pulse, the continuation of the pulse resulted in a positively skewed distribution of ΔERKTR at frame $t + 1$ (Fig. 5*D*). In contrast, in a non-thresholded population of cells, the distribution of ΔERKTR was centered around 0, reflecting the fact that at any given time, most cells are not undergoing a pulse (Fig. 5*D*, *gray distribution*). This signature has practical significance because it allows the rising phase of the ERK activity pulse to be detected reliably over multiple time points. With either reporter alone, detecting the rising phase reliably at subsequent time points would involve a tradeoff between sampling frequency and the size of the increase detected at each interval (with a higher frequency resulting in smaller, less easily detected changes). The two-reporter strategy allows for a more reliable detection even in the context of substantial variability in pulse shapes.

To first establish that EGFR inhibition by gefitinib occurs rapidly enough to halt pulse continuation, we treated cells under high (20 ng/ml) EGF stimulation with gefitinib. A decrease in EKAR3 was detectable at the second time point following the addition of the drug, a latency of ~3 min (Fig. 6*A*). Thus, binding of gefitinib to EGFR within cells is potentially fast enough to arrest EGFR activity in the midst of the 10-min amplification phase. We next tracked a population of cells undergoing spontaneous pulses at a range of low EGF concentrations (0.02–0.1 ng/ml); upon treatment with gefitinib, we observed an immediate cessation of new pulses (Fig. 6*A*).

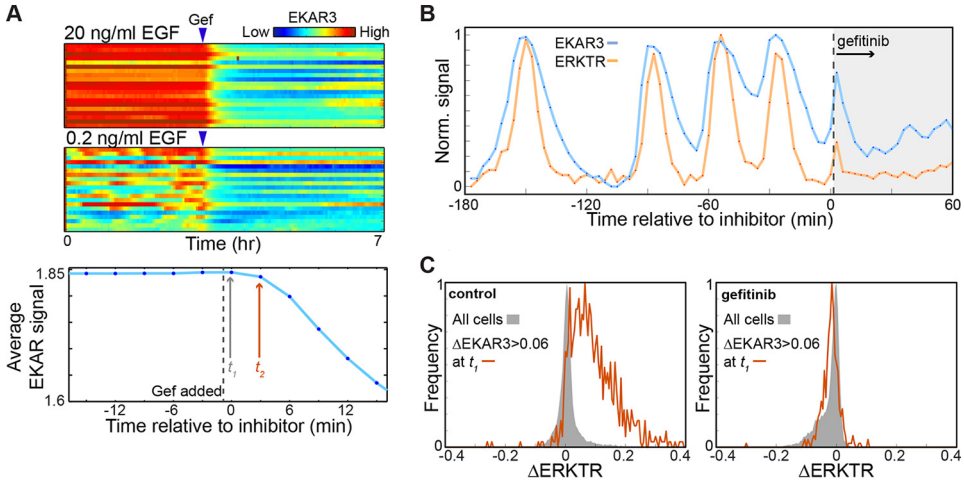

FIGURE 6. **Requirement of continuous EGFR activity during ERK activity pulses.** *A*, kinetics of ERK inhibition by gefitinib. *Top*, heat maps of MCF10A-EKAR3 cells exposed to high or low EGF and treated with 1 μM gefitinib at the indicated time. *Bottom*, average EKAR3 signal for 500 cells following gefitinib treatment in the presence of 20 ng/ml EGF. The point marked t_1 indicates the first time point following gefitinib application, whereas t_2 indicates the first time point at which a reduction in EKAR3 signal is detectable, indicating sufficient binding of gefitinib to inhibit EGFR. *B*, representative EKAR3 and ERKTR responses in an individual cell treated with 1 μM gefitinib during a spontaneous ERK activity pulse (stimulated by 0.02 ng/ml EGF). *C*, pulse continuation signatures in the presence of gefitinib. Cells cultured in the presence of 0.1, 0.05, or 0.02 ng/ml EGF were imaged and treated with gefitinib as in *A*, or mock-treated. Distributions of ΔERKTR at t_2 are shown for all cells (*gray*) or for cells with above-threshold ΔEKAR3 at t_1 (*orange*). Data shown were pooled from all three EGF concentrations.

To examine the immediate effect of gefitinib on already-initiated pulses, we first determined the characteristic pulse amplitude for each cell based on its ERK activity profile prior to gefitinib treatment. We manually searched 2000 cells to identify those that, at the time of gefitinib addition, had initiated a pulse but not yet reached their characteristic peak. We identified 22 cells in this category, and all 22 of these cells failed to reach the expected peak amplitude following EGFR inhibition (Fig. 6*B*).

To confirm the effect of EGFR inhibition on nascent pulses in an unbiased manner, we examined the signature of EKAR3-ERKTR ordering described in Fig. 5*D*. We focused on two time points following drug treatment: t_1, immediately following drug addition and before the gefitinib had entered the cells, and t_2, the first point at which gefitinib effects could be observed in control experiments (Fig. 6*A*). In vehicle-treated conditions, cells with a high ΔEKAR3 at t_1 also had a high ΔERKTR at t_2, reflecting the continuation of the ERK activity pulse, as in unperturbed conditions (Fig. 6*C*; compare with Fig. 5*D*). However, in gefitinib-treated cells, the positive skew of ΔERKTR at t_2 was completely eliminated, indicating that all ongoing pulses were effectively terminated by EGFR inhibition. Therefore, we conclude that EGFR kinase activity is required to maintain ERK kinase activity for the entire duration of each ERK activity pulse.

Discussion

The data presented here substantially reduce the number of candidate mechanisms that may drive the "on" phase of ERK activity pulses in EGF-stimulated cells. The majority of computational models of bimodal, oscillatory, or positive feedback-driven ERK activity have focused on events within the core Ras-Raf-MEK-ERK cascade (14, 23, 24, 36–39). However, our data indicate that these events are not the operative mechanism underlying EGF-driven ERK activity pulses in MCF10A cells. Core pathway mechanisms, such as feedback loops 2, 3, and 4 (Fig. 1*A*), would allow bimodal or "digital" ERK activity pulses to be generated irrespective of the initiating receptor and to continue independently of receptor activity once initiated. In contrast, we observe that different receptor systems drive distinct modes of ERK activity and that EGF-induced pulses remain continuously dependent on receptor activity. Our data do not rule out the possibility that the core loops are present and influence dynamics under some conditions but do indicate that these loops are not strong enough to generate bimodal ERK activity under all circumstances.

We suggest that receptor level feedback or cooperativity is the element that enforces uniform ERK activation within every EGF-stimulated pulse to create a "dynamically digital" time-dependent response. Feedback loop 1, in which Ras-GTP allosterically activates the exchange factor activity of SOS, is one candidate for this mechanism. Because both EGFR and TrkA are capable of signaling through SOS, this possibility would require a differential affinity of the two receptors for SOS, which has been observed (34). This feedback loop has previously been implicated in driving digital ERK activation in lymphocytes using fixed cell measurements to assay the initial stimulus response (40). Our data also do not exclude mechanisms of cooperativity in the physical assembly of receptor complexes within membrane subregions (41, 42), or positive feedback through stimulated release of autocrine EGFR ligands (43).

Our experiments suggest non-saturating amplification of upstream signals by the Ras-Raf-MEK-ERK cascade in MCF10A, non-tumor cells that contain no known mutations in the Ras network. Although TrkA is not a native component of the pathway within these cells, its ability to stimulate amplitude-modulated ERK activity indicates that the core pathway is capable of responding in a graded manner to at least some receptor inputs. This graded response is consistent with recent findings in which direct optogenetic activation of Ras results in a linearly amplified level of ERK activity (44); however, our measurements are unique in demonstrating that both amplitude-

and frequency-modulated signaling can occur within the same cellular system.

A complicating factor in comparing TrkA and EGFR responses is the differential activation of Rap1 by NGF and EGF (35); Rap-1 signals more strongly through B-Raf, whereas Ras acts preferentially through c-Raf (45, 46). Because it is unclear whether feedback loops 3 and 4 operate equivalently on c-Raf or B-Raf, it cannot be concluded from the NGF-TrkA experiment alone that these loops are not involved in pulse generation. However, because our inhibitor studies demonstrate that the EGFR-driven cascade relies on continued receptor activity to reach full ERK activation, the most parsimonious model is that the core Ras-Raf-MEK-ERK cascade performs linearly in both NGF and EGF cases, with the difference in dynamic properties being restricted to the receptor level.

How do the single-cell data reported here compare with published data for population averages of ERK activity in response to EGF and NGF stimulation (45)? EGF-stimulated ERK activity, measured by immunoblot for phosphorylated ERK (pERK), is typically reported to peak within 10–30 min following EGF stimulation and then to decay rapidly; in some cases, a second, sustained period of attenuated ERK activity follows (47, 48). A notable difference between this stereotypical profile and the single-cell data presented here is the lack of a pronounced decline following the initial increase. A potential explanation for this difference is that measurements of enzymatic substrates (such as the EKAR3 or ERKTR reporters) may differ from direct quantification of the active enzyme (pERK), particularly when enzyme activity is high enough to exhaust the substrate (49). It is possible that high ERK activity saturates the reporter during the early phase of activation, resulting in an underestimate of the initial peak height (relative to measurements of pERK). Consistent with this explanation, the initial round of EGF-stimulated ERK nuclear translocation, an indicator of its activity, has been shown to be more complete than subsequent pulses in the same cell (50). Additional improvements in ERK activity reporters may be needed to extend their dynamic range to capture both low- and high-amplitude events faithfully.

In our system, the second phase of ERK activity consists of sporadic, asynchronous pulses, which, averaged over many cells, create the appearance of a steady, sustained response. The observed pERK signal in this phase varies between published studies using population level measurements, with some reporting a rapid down-regulation of pERK in MCF10A cells stimulated with saturating EGF (48, 51) and others reporting a more sustained response (52, 53). We attribute these differences to variation in the frequency at which EGFR is restimulated, either by the continuous presence of EGF or by autocrine EGF ligand signaling. Potential sources of variation that could affect this frequency include 1) differences in experimental culture volume, which can affect the amount of EGF available to cells due to rapid internalization of the ligand (54); 2) the local density of the cells being imaged, with pulses occurring less frequently in denser regions of the monolayer (14); and 3) differences between strains of MCF10A cells in their sensitivity to EGF or propensity for autocrine signaling.[3] Studies in which the second wave of ERK activity is weak may represent instances in which negative feedback is particularly strong, autocrine EGF ligand secretion is absent, and/or EGF depletion from the medium is rapid.

Sustained responses observed at the population level may reflect either true continuous activity of ERK at the single cell level or the presence of asynchronous pulses, and single-cell data are needed to eliminate this ambiguity. In demonstrating that EGF leads to discrete (although often asynchronous) ERK pulses at the single cell level, whereas NGF results in true sustained activity, our data indicate that single-cell behavior is in fact largely consistent with the "classical" model of EGF and NGF producing transient or sustained ERK activity, respectively. Similarly, our data provide the resolution to confirm that rapid loss of ERK activity upon EGFR inhibition (55) results from premature termination of existing pulses rather than simply blocking initiation of new pulses.

Our findings contrast at several points with findings made by fixed cell measurement. Bimodal, rather than graded, ERK responses have been observed in NGF-stimulated PC-12 cells (56), whereas we observe constant, graded signaling in response to NGF. In 3T3 cells, staining of phosphorylated ERK appears to be amplitude-modulated upon stimulation with serum but bimodal when activated by an inducible version of Raf (57), suggesting a downstream origin for bimodal responses. These disparities may reflect differences between the cell types under study or may reflect the drawbacks of fixed cell methods (9). The dual-reporter strategy reported here should provide the reliability and temporal resolution to accurately resolve the single-cell kinetics in these systems.

Because of its central role in cell regulation, the EGFR-Ras-ERK pathway has become a model for systems biology studies that aim to model the duration and amplitude of ERK activity and the resulting cellular response. Single-cell data are valuable in model construction because of their ability to resolve changes in kinetics that would be obscured in population average data (58). Also important will be identification of the negative feedbacks driving the deactivation phase of pulses. Although negative feedback loops involved in EGFR signaling have been systematically assessed (18), single-cell experiments will be needed to determine which mechanisms operate within each pulse to terminate ERK activity and which attenuate overall pulse frequency. Together, these data will allow more accurate modeling of the kinetics of ERK activity in response to receptor tyrosine kinase stimulation.

Author Contributions—B. S. established the MCF10A-TrkA experimental system and performed the experiments shown in Figs. 3–6. M. P. and M. M. constructed and validated the EKAR3 reporter used in Figs. 2–6. G. B. constructed the dual ERK reporter cell line used in Figs. 5 and 6. K. D. performed image analysis and data extraction for Figs. 2–6. J. G. A. conceived and coordinated the study and wrote the paper. All authors reviewed the results and edited and approved the final version of the manuscript.

Acknowledgments—We thank K. Aoki and M. Matsuda for the EKAR-EV biosensor, S. Regot and M. Covert for the ERKTR biosensor, and Sean Collins and members of the Albeck and Collins laboratories for helpful discussions.

References

1. Yoon, S., and Seger, R. (2006) The extracellular signal-regulated kinase: multiple substrates regulate diverse cellular functions. *Growth Factors* **24,** 21–44
2. Marshall, C. J. (1995) Specificity of receptor tyrosine kinase signaling: transient *versus* sustained extracellular signal-regulated kinase activation. *Cell* **80,** 179–185
3. Murphy, L. O., MacKeigan, J. P., and Blenis, J. (2004) A network of immediate early gene products propagates subtle differences in mitogen-activated protein kinase signal amplitude and duration. *Mol. Cell Biol.* **24,** 144–153
4. Murphy, L. O., Smith, S., Chen, R. H., Fingar, D. C., and Blenis, J. (2002) Molecular interpretation of ERK signal duration by immediate early gene products. *Nat. Cell Biol.* **4,** 556–564
5. Jones, S. M., and Kazlauskas, A. (2001) Growth-factor-dependent mitogenesis requires two distinct phases of signalling. *Nat. Cell Biol.* **3,** 165–172
6. Zwang, Y., Sas-Chen, A., Drier, Y., Shay, T., Avraham, R., Lauriola, M., Shema, E., Lidor-Nili, E., Jacob-Hirsch, J., Amariglio, N., Lu, Y., Mills, G. B., Rechavi, G., Oren, M., Domany, E., and Yarden, Y. (2011) Two phases of mitogenic signaling unveil roles for p53 and EGR1 in elimination of inconsistent growth signals. *Mol. Cell* **42,** 524–535
7. Kwong, L. N., Costello, J. C., Liu, H., Jiang, S., Helms, T. L., Langsdorf, A. E., Jakubosky, D., Genovese, G., Muller, F. L., Jeong, J. H., Bender, R. P., Chu, G. C., Flaherty, K. T., Wargo, J. A., Collins, J. J., and Chin, L. (2012) Oncogenic NRAS signaling differentially regulates survival and proliferation in melanoma. *Nat. Med.* **18,** 1503–1510
8. Purvis, J. E., and Lahav, G. (2013) Encoding and decoding cellular information through signaling dynamics. *Cell* **152,** 945–956
9. Birtwistle, M. R., Rauch, J., Kiyatkin, A., Aksamitiene, E., Dobrzyński, M., Hoek, J. B., Kolch, W., Ogunnaike, B. A., and Kholodenko, B. N. (2012) Emergence of bimodal cell population responses from the interplay between analog single-cell signaling and protein expression noise. *BMC Syst. Biol.* **6,** 109
10. Komatsu, N., Aoki, K., Yamada, M., Yukinaga, H., Fujita, Y., Kamioka, Y., and Matsuda, M. (2011) Development of an optimized backbone of FRET biosensors for kinases and GTPases. *Mol. Biol. Cell* **22,** 4647–4656
11. Harvey, C. D., Ehrhardt, A. G., Cellurale, C., Zhong, H., Yasuda, R., Davis, R. J., and Svoboda, K. (2008) A genetically encoded fluorescent sensor of ERK activity. *Proc. Natl. Acad. Sci. U.S.A.* **105,** 19264–19269
12. Regot, S., Hughey, J. J., Bajar, B. T., Carrasco, S., and Covert, M. W. (2014) High-sensitivity measurements of multiple kinase activities in live single cells. *Cell* **157,** 1724–1734
13. Albeck, J. G., Mills, G. B., and Brugge, J. S. (2013) Frequency-modulated pulses of ERK activity transmit quantitative proliferation signals. *Mol. Cell* **49,** 249–261
14. Aoki, K., Kumagai, Y., Sakurai, A., Komatsu, N., Fujita, Y., Shionyu, C., and Matsuda, M. (2013) Stochastic ERK activation induced by noise and cell-to-cell propagation regulates cell density-dependent proliferation. *Mol. Cell* **52,** 529–540
15. Hiratsuka, T., Fujita, Y., Naoki, H., Aoki, K., Kamioka, Y., and Matsuda, M. (2015) Intercellular propagation of extracellular signal-regulated kinase activation revealed by *in vivo* imaging of mouse skin. *Elife* **4,** e05178
16. Cai, L., Dalal, C. K., and Elowitz, M. B. (2008) Frequency-modulated nuclear localization bursts coordinate gene regulation. *Nature* **455,** 485–490
17. Hao, N., Budnik, B. A., Gunawardena, J., and O'Shea, E. K. (2013) Tunable signal processing through modular control of transcription factor translocation. *Science* **339,** 460–464
18. Cirit, M., Wang, C. C., and Haugh, J. M. (2010) Systematic quantification of negative feedback mechanisms in the extracellular signal-regulated kinase (ERK) signaling network. *J. Biol. Chem.* **285,** 36736–36744
19. Boykevisch, S., Zhao, C., Sondermann, H., Philippidou, P., Halegoua, S., Kuriyan, J., and Bar-Sagi, D. (2006) Regulation of ras signaling dynamics by Sos-mediated positive feedback. *Curr. Biol.* **16,** 2173–2179
20. Margarit, S. M., Sondermann, H., Hall, B. E., Nagar, B., Hoelz, A., Pirruccello, M., Bar-Sagi, D., and Kuriyan, J. (2003) Structural evidence for feedback activation by Ras.GTP of the Ras-specific nucleotide exchange factor SOS. *Cell* **112,** 685–695
21. Balan, V., Leicht, D. T., Zhu, J., Balan, K., Kaplun, A., Singh-Gupta, V., Qin, J., Ruan, H., Comb, M. J., and Tzivion, G. (2006) Identification of novel in vivo Raf-1 phosphorylation sites mediating positive feedback Raf-1 regulation by extracellular signal-regulated kinase. *Mol. Biol. Cell* **17,** 1141–1153
22. Marchetti, S., Gimond, C., Chambard, J. C., Touboul, T., Roux, D., Pouysségur, J., and Pagès, G. (2005) Extracellular signal-regulated kinases phosphorylate mitogen-activated protein kinase phosphatase 3/DUSP6 at serines 159 and 197, two sites critical for its proteasomal degradation. *Mol. Cell Biol.* **25,** 854–864
23. Shin, S. Y., Rath, O., Choo, S. M., Fee, F., McFerran, B., Kolch, W., and Cho, K. H. (2009) Positive- and negative-feedback regulations coordinate the dynamic behavior of the Ras-Raf-MEK-ERK signal transduction pathway. *J. Cell Sci.* **122,** 425–435
24. Shin, S. Y., Rath, O., Zebisch, A., Choo, S. M., Kolch, W., and Cho, K. H. (2010) Functional roles of multiple feedback loops in extracellular signal-regulated kinase and Wnt signaling pathways that regulate epithelial-mesenchymal transition. *Cancer Res.* **70,** 6715–6724
25. Janes, K. A., Wang, C. C., Holmberg, K. J., Cabral, K., and Brugge, J. S. (2010) Identifying single-cell molecular programs by stochastic profiling. *Nat. Methods* **7,** 311–317
26. Jaqaman, K., Loerke, D., Mettlen, M., Kuwata, H., Grinstein, S., Schmid, S. L., and Danuser, G. (2008) Robust single-particle tracking in live-cell time-lapse sequences. *Nat. Methods* **5,** 695–702
27. Birtwistle, M. R., von Kriegsheim, A., Kida, K., Schwarz, J. P., Anderson, K. I., and Kolch, W. (2011) Linear approaches to intramolecular Forster resonance energy transfer probe measurements for quantitative modeling. *PLoS One* **6,** e27823
28. Goedhart, J., von Stetten, D., Noirclerc-Savoye, M., Lelimousin, M., Joosen, L., Hink, M. A., van Weeren, L., Gadella, T. W., Jr., and Royant, A. (2012) Structure-guided evolution of cyan fluorescent proteins towards a quantum yield of 93%. *Nat. Commun.* **3,** 751
29. Bessman, N. J., Bagchi, A., Ferguson, K. M., and Lemmon, M. A. (2014) Complex relationship between ligand binding and dimerization in the epidermal growth factor receptor. *Cell Rep.* **9,** 1306–1317
30. Blinov, M. L., Faeder, J. R., Goldstein, B., and Hlavacek, W. S. (2006) A network model of early events in epidermal growth factor receptor signaling that accounts for combinatorial complexity. *Biosystems* **83,** 136–151
31. Lemmon, M. A., and Schlessinger, J. (2010) Cell signaling by receptor tyrosine kinases. *Cell* **141,** 1117–1134
32. Vanhecke, E., Adriaenssens, E., Verbeke, S., Meignan, S., Germain, E., Berteaux, N., Nurcombe, V., Le Bourhis, X., and Hondermarck, H. (2011) Brain-derived neurotrophic factor and neurotrophin-4/5 are expressed in breast cancer and can be targeted to inhibit tumor cell survival. *Clin. Cancer Res.* **17,** 1741–1752
33. Kang, B. H., Jensen, K. J., Hatch, J. A., and Janes, K. A. (2013) Simultaneous profiling of 194 distinct receptor transcripts in human cells. *Sci. Signal.* **6,** rs13
34. Basu, T., Warne, P. H., and Downward, J. (1994) Role of Shc in the activation of Ras in response to epidermal growth factor and nerve growth factor. *Oncogene* **9,** 3483–3491
35. Kao, S., Jaiswal, R. K., Kolch, W., and Landreth, G. E. (2001) Identification of the mechanisms regulating the differential activation of the mapk cascade by epidermal growth factor and nerve growth factor in PC12 cells. *J. Biol. Chem.* **276,** 18169–18177
36. Kholodenko, B. N. (2000) Negative feedback and ultrasensitivity can bring about oscillations in the mitogen-activated protein kinase cascades. *Eur. J. Biochem.* **267,** 1583–1588
37. Markevich, N. I., Hoek, J. B., and Kholodenko, B. N. (2004) Signaling switches and bistability arising from multisite phosphorylation in protein kinase cascades. *J. Cell Biol.* **164,** 353–359
38. Chickarmane, V., Kholodenko, B. N., and Sauro, H. M. (2007) Oscillatory dynamics arising from competitive inhibition and multisite phosphorylation. *J. Theor. Biol.* **244,** 68–76
39. Blüthgen, N., Bruggeman, F. J., Legewie, S., Herzel, H., Westerhoff, H. V., and Kholodenko, B. N. (2006) Effects of sequestration on signal transduction cascades. *FEBS J.* **273,** 895–906

40. Das, J., Ho, M., Zikherman, J., Govern, C., Yang, M., Weiss, A., Chakraborty, A. K., and Roose, J. P. (2009) Digital signaling and hysteresis characterize ras activation in lymphoid cells. *Cell* **136,** 337–351
41. James, J. R., and Vale, R. D. (2012) Biophysical mechanism of T-cell receptor triggering in a reconstituted system. *Nature* **487,** 64–69
42. Ariotti, N., Liang, H., Xu, Y., Zhang, Y., Yonekubo, Y., Inder, K., Du, G., Parton, R. G., Hancock, J. F., and Plowman, S. J. (2010) Epidermal growth factor receptor activation remodels the plasma membrane lipid environment to induce nanocluster formation. *Mol. Cell Biol.* **30,** 3795–3804
43. Shvartsman, S. Y., Hagan, M. P., Yacoub, A., Dent, P., Wiley, H. S., and Lauffenburger, D. A. (2002) Autocrine loops with positive feedback enable context-dependent cell signaling. *Am. J. Physiol. Cell Physiol.* **282,** C545–C559
44. Toettcher, J. E., Weiner, O. D., and Lim, W. A. (2013) Using optogenetics to interrogate the dynamic control of signal transmission by the ras/erk module. *Cell* **155,** 1422–1434
45. Sasagawa, S., Ozaki, Y., Fujita, K., and Kuroda, S. (2005) Prediction and validation of the distinct dynamics of transient and sustained ERK activation. *Nat. Cell Biol.* **7,** 365–373
46. Zhou, Y., and Hancock, J. F. (2015) Ras nanoclusters: versatile lipid-based signaling platforms. *Biochim. Biophys. Acta* **1853,** 841–849
47. Chen, W. W., Schoeberl, B., Jasper, P. J., Niepel, M., Nielsen, U. B., Lauffenburger, D. A., and Sorger, P. K. (2009) Input-output behavior of ErbB signaling pathways as revealed by a mass action model trained against dynamic data. *Mol. Syst. Biol.* **5,** 239
48. Niepel, M., Hafner, M., Pace, E. A., Chung, M., Chai, D. H., Zhou, L., Schoeberl, B., and Sorger, P. K. (2013) Profiles of Basal and stimulated receptor signaling networks predict drug response in breast cancer lines. *Sci. Signal.* **6,** ra84
49. Fujita, Y., Komatsu, N., Matsuda, M., and Aoki, K. (2014) Fluorescence resonance energy transfer based quantitative analysis of feedforward and feedback loops in epidermal growth factor receptor signaling and the sensitivity to molecular targeting drugs. *FEBS J.* **281,** 3177–3192
50. Cohen-Saidon, C., Cohen, A. A., Sigal, A., Liron, Y., and Alon, U. (2009) Dynamics and variability of ERK2 response to EGF in individual living cells. *Mol. Cell* **36,** 885–893
51. Brummer, T., Schramek, D., Hayes, V. M., Bennett, H. L., Caldon, C. E., Musgrove, E. A., and Daly, R. J. (2006) Increased proliferation and altered growth factor dependence of human mammary epithelial cells overexpressing the Gab2 docking protein. *J. Biol. Chem.* **281,** 626–637
52. Tang, W. Y., Beckett, A. J., Prior, I. A., Coulson, J. M., Urbé, S., and Clague, M. J. (2014) Plasticity of mammary cell boundaries governed by EGF and actin remodeling. *Cell Rep.* **8,** 1722–1730
53. Graham, N. A., and Asthagiri, A. R. (2004) Epidermal growth factor-mediated T-cell factor/lymphoid enhancer factor transcriptional activity is essential but not sufficient for cell cycle progression in nontransformed mammary epithelial cells. *J. Biol. Chem.* **279,** 23517–23524
54. Knauer, D. J., Wiley, H. S., and Cunningham, D. D. (1984) Relationship between epidermal growth factor receptor occupancy and mitogenic response: quantitative analysis using a steady state model system. *J. Biol. Chem.* **259,** 5623–5631
55. Kleiman, L. B., Maiwald, T., Conzelmann, H., Lauffenburger, D. A., and Sorger, P. K. (2011) Rapid phospho-turnover by receptor tyrosine kinases impacts downstream signaling and drug binding. *Mol. Cell* **43,** 723–737
56. Santos, S. D., Verveer, P. J., and Bastiaens, P. I. (2007) Growth factor-induced MAPK network topology shapes Erk response determining PC-12 cell fate. *Nat. Cell Biol.* **9,** 324–330
57. Sturm, O. E., Orton, R., Grindlay, J., Birtwistle, M., Vyshemirsky, V., Gilbert, D., Calder, M., Pitt, A., Kholodenko, B., and Kolch, W. (2010) The mammalian MAPK/ERK pathway exhibits properties of a negative feedback amplifier. *Sci. Signal.* **3,** ra90
58. Ahmed, S., Grant, K. G., Edwards, L. E., Rahman, A., Cirit, M., Goshe, M. B., and Haugh, J. M. (2014) Data-driven modeling reconciles kinetics of ERK phosphorylation, localization, and activity states. *Mol. Syst. Biol.* **10,** 718